Nonlinear Rock Mechanics

Chapter · January 2006

DOI: 10.1007/978-0-387-35851-2_5

1 author:

G. Exadaktylos
National Technical University of Athens
88 PUBLICATIONS **1,723** CITATIONS

SEE PROFILE

5

Nonlinear Rock Mechanics

G.E. Exadaktylos

Mining Design Laboratory, Department of Mineral Resources Engineering Department, Technical University of Crete, University Campus, Akrotiri GR-73100, Chania, Greece, Tel: +30 28210 37690, Fax: +30 28210 37891, e-mail: exadakty@mred.tuc.gr, http://minelab.mred.tuc.gr.

Abstract
Rock mechanics is a rapidly evolving scientific discipline that is concerned with the development of experimental and theoretical tools to study and predict the behavior of intact (or damaged) and discontinuous (fractured) rocks under the influence of chemo-thermo-poro-mechanical effects under static or dynamic conditions. Nonlinearity is inherent in many rock mechanical problems. Some indicative examples are briefly listed herein. In physical nonlinearity, few, if any, rocks are truly "elastic" and even fewer are "linear" or "Hookean." Natural or stress-induced nonlinear directional response (anisotropy) is possible. In addition, coupled thermal, fluid flow, and mechanical effects or processes may give considerable nonlinearities in the response of porous rocks. In geometric nonlinearity, many structures undergo very large deformations in normal or in damaged conditions (e.g., buildings and other manmade structures after major earthquakes (See chapter 4)). In constraints, nonlinearity, contact between deformable rocks (e.g., contact of lips of faults), or rock structure may occur such that the common surface is unknown. A central point of any rock mechanical problem is the constitutive description of the rock. In this chapter the basic ingredients of a nonlinear constitutive mechanical theory for rocks based on experimental evidence is outlined and tested by exploiting triaxial compression experiments of a sandstone.

Keywords: Damage, fracture mechanics, hypoelasticity, Mohr–Coulomb, nonlinearity, plasticity, rocks, sandstone, triaxial compression

1. Introduction

Rocks are granular, porous, heterogeneous, anisotropic natural materials formed under certain geological processes (i.e., sedimentary, magmatic, or metamorphic) during a rather extended (geological) time scale (Figures 5.1a,b), hence their behavior is more complex as compared to concretes, ceramics, metals, and other manmade materials. Rocks are composed of a vast variety of minerals and occur in an almost infinite range of conditions, from crystalline solids to aggregations of independent particles. In general, rocks exhibit elasticity, plasticity, damage (Van den Abeele and Windels, this volume), cracking, elastic hysteresis, and memory (Pascualini, this volume;

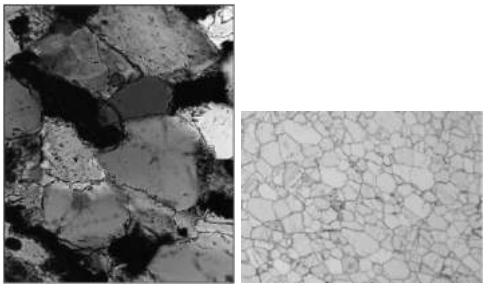

Fig. 5.1. Typical granular microstructure (fabric) of rocks observed with an optical microscope: (a) heterogeneous Berea sandstone with pores and microcracks (Guyer and Johnson, 1999) and (b) low porosity homogeneous Gioia marble rock microstructure with twins in calcite crystals (courtesy of P. Tiano).

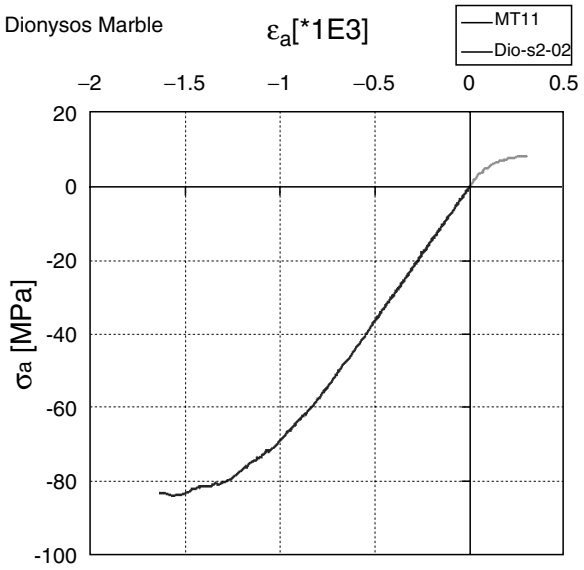

Fig. 5.2. Typical axial stress–axial strain curve of a rock in uniaxial tension–compression (Dionysos marble) (courtesy of I. Vardoulakis).

TenCate et al., this volume), dilatancy, creep, pressure, and rate dependency, nonequilibrium nonlinear dynamics (Johnson, this volume; TenCate et al., this volume), size effects, and anisotropy, among others. Another important property of geologic materials that is attributed to the presence of healed or open microcracks, pore topology, and other defects such as soft inclusions, is that their uniaxial tensile strength is much smaller (one order of magnitude) than their uniaxial compressive strength (Figure 5.2). This is a clear manifestation of "brittleness." The convention of positive tension and elongation is assumed unless stated otherwise.

Due to all these phenomena that accompany rock mechanical behavior, modern rock mechanics should rely upon all the up-to-date developments of the fundamental theories of continuum and discontinuum mechanics, elasticity, strength of materials, damage mechanics, plasticity, and fracture mechanics in order to present robust models

for rocks subjected to static or to dynamic loads. The linking of all these theories under the umbrella of a unique theory capable of describing the rock mechanical behavior at all scales (i.e., in the range of 1e 6 m to 1e 4 m) and boundary conditions encountered in practice, is one of the fascinating challenges of the future.

In the following paragraphs a brief account of nonlinearities accompanying rock behavior under static mechanical loads is given, and an example of calibration of a new nonlinear mechanical model on a series of uniaxial and triaxial compression experimental data of a heterogeneous sandstone is illustrated.

2. Elasticity and Plasticity of Rocks

The study of the elasticity of rocks is the first step towards the construction of robust models. For easy reference a few definitions and basic properties of elastic, hyper-, and hypoelastic constitutive equations are mentioned in this section [for an extensive review see (Truesdell and Noll, 1965; Chen nad Han, 1988; Vardoulakis and Sulem, 1995)]. A material is called *elastic* if: (a) it possesses only one ground state, that is, a state that is undeformed and is also stress-free, and if (b) the stress σ_{ij} is a function of the deformation gradient or strain $\varepsilon_{kl}^{(el)}$, that is,

$$\sigma_{ij} = T_{ij}\left(\varepsilon_{kl}^{(el)}\right), \qquad i, j, k, l = 1, 2, 3, \tag{5.1}$$

wherein superscript (el) indicates elastic strains and the usual notation and rules for tensors are followed (e.g., Frederick and Chang, 1972). The elastic material defined by (5.1) is called a "Cauchy elastic material." From this equation we observe that in *closed stress paths* in stress space elastic materials are characterized by zero residual strain. In the small-strain linear Cauchy elasticity in isothermal or adiabatic conditions, the stress–strain relationship may be stated in the following way,

$$\sigma_{ij} = C_{ijkl}\varepsilon_{kl}^{(el)}, \qquad C_{ijkl} = \text{constants} \tag{5.2}$$

More restrictive is the definition of the *hyperelastic* or Green elastic materials. In hyperelasticity we postulate a strain energy density function

$$w^{(el)} = w^{(el)}(\varepsilon_{ij}^{(el)}) \tag{5.3}$$

such that,

$$\sigma_{ij} = \frac{\partial w^{(el)}}{\partial \varepsilon_{ij}^{(el)}}. \tag{5.4}$$

The above relationship means that the stress tensor is derived from the gradient of the strain potential function, or alternatively that the stress is normal to the surface $w^{(el)} = const$. Thus we conclude that equation Eq. (5.2) for isotropic elastic materials follows from the form (5.4) for hyperelastic materials. The converse is not generally true. If the material is hyperelastic along a closed strain path the total specific work done by the stresses is null. This is not generally true for (Cauchy) elastic materials. However, in closed stress paths in stress space both elastic materials and hyperelastic

materials are characterized by zero residual strain. We observe that both the constitutive equations of isotropic elastic materials 5.3 and for isotropic hyperelastic materials (5.6) lead through formal material time-differentiation to equations of the rate form

$$\dot{\sigma}_{ij} = C^{(el)}_{ijkl}\dot{\varepsilon}^{(el)}_{kl}, \tag{5.5}$$

where the dot indicates differentiation w.r.t. time. Truesdell and Noll (1965) defined a class of materials, which they call "hypoelastic materials", that obey rate constitutive equations like the one above, which are linear in $\dot{\varepsilon}^{(el)}_{ij}$, with the additional restriction that the corresponding fourth-order constitutive tensor is an isotropic tensor function of the stress. Hypoelastic constitutive models are used to describe the mechanical behavior of a class of materials in which the state of stress depends on the current state of strain as well as on the stress path followed to reach that state. Hypoelasticity equations are derived from hyperelasticity. In general, however, hypoelastic constitutive equations are neither integrable to a finite form (5.1) nor connected to a strain energy function through a constitutive equation of the form of (5.4). Thus, hypoelastic equations will lead in general to residual strain, if integrated along closed stress paths, and to violations of the second law of thermodynamics if integrated along closed strain paths.

In elastoplastic constitutive equations it is often assumed that the background elasticity is a Hooke-hypoelasticity; that is,

$$C^{(el)}_{ijkl} = G\left\{\delta_{ik}\delta_{jl} + \delta_{il}\delta_{jk} + \frac{2\nu}{1-2\nu}\delta_{ij}\delta_{kl}\right\} \tag{5.6}$$

with constant secant shear modulus G and constant secant Poisson's ratio ν, where δ_{ik} is the Kronecker delta. The next modeling step is based on the study of rock plasticity and strength. Incremental plasticity theory is based on a few fundamental postulates. Plasticity models are written as rate-independent models or as rate-dependent models. A rate-independent model is one in which the constitutive response does not depend on the rate of deformation: the response of many rocks at low temperatures relative to their melting temperature and at low strain rates is effectively rate independent. In a rate-dependent model the response does depend on the rate at which the material is strained. Examples of such models are the simple "creep" models and the rate-dependent plasticity model that is used to describe the behavior of rocks at higher strain rates. Because these models have similar forms, their numerical treatment is based on the same technique. A basic assumption of elastic–plastic models is that the deformation can be divided into an elastic part and an inelastic (plastic) part. This decomposition can be used directly to formulate the plasticity model. Historically, an additive strain rate decomposition is employed (Hill, 1950),

$$\dot{\varepsilon}_{ij} = \dot{\varepsilon}^{(el)}_{ij} + \dot{\varepsilon}^{(pl)}_{ij}, \tag{5.7}$$

where the superscript pl indicates plastic strains. For rate-independent materials we may use instead of the rate of deformation the incremental deformation; that is,

$$\Delta\varepsilon_{ij} = \dot{\varepsilon}_{ij}. \tag{5.8}$$

The elastic part of the response is assumed to be derivable from an elastic model presented previously. The cohesional, frictional, and dilatational properties of rocks up to failure may be modeled within the frame of elastoplasticity theory with strain-hardening yield surface and nonassociative flow rule. The yield surface F that defines the limit to this region of purely elastic response and plastic potential Q that defines the plastic part of strain may be expressed as follows,

$$F = F\left(\sigma_{ij}, \psi\right), \quad Q = Q\left(\sigma_{ij}, \psi\right), \tag{5.9}$$

in which ψ denotes a hardening parameter, that is, a measure of plastic deformation. The hardening parameter or parameters are state variables that are introduced to allow the models to describe some of the complexity of the inelastic response of real materials. In the simplest plasticity model (*perfect plasticity*) the yield surface acts as a limit surface and there are no hardening parameters at all: no part of the model evolves during the deformation. Complex plasticity models usually include a large number of hardening parameters.

Plastic strain rates are generated when the state of stress lies on the yield surface and if loading of that yield surface is taking place, that is to say, the following "consistency criterion" is satisfied,

$$F = 0, \qquad \dot{F} > 0, \quad \text{and } \dot{\psi} > 0. \tag{5.10}$$

When the material is flowing inelastically the inelastic part of the deformation is defined by the flow rule, which we can write in incremental form as follows,[1]

$$\Delta\varepsilon_{ij}^{(pl)} = \Delta\psi \frac{\partial Q}{\partial \sigma_{ij}}, \quad \psi \geq 0. \tag{5.11}$$

The rate form of the flow rule is essential to incremental plasticity theory, because it allows the history dependence of the response to be modeled. The plastic potential and the yield function may be identical, that is, $Q = F$, only if the measured dilatation and strength responses of rock are identical. Such models are called *associated flow* plasticity models. Associated flow models are useful for materials in which dislocation motion provides the fundamental mechanisms of plastic flow when there are no sudden changes in the direction of the plastic strain rate at a point. They are generally not accurate for materials in which the inelastic deformation is primarily caused by frictional mechanisms as in the case for geomaterials. For a plastic potential that is an isotropic function of the stress tensor, Eq. (5.11) describes a *co-axial flow rule*; that is, the principal axes of plastic strain rate coincide with the principal axes of stress.

The feature that distinguishes the inelastic behavior of nonmetallic porous materials, such as concrete, rocks, and soils, from that of metals is the occurrence of plastic volume changes. Metals undergo no change in volume as a result of plastic deformation. Rocks, on the other hand, may either dilate (increase in volume) or compact (decrease in volume) as a result of plastic deformation. From the macroscopic point of view and

[1] The inequality $\psi \geq 0$ is essential in plasticity and defines the irreversible character of plastic deformations.

for granular media under shear, irreversible shear strains $g^{(pl)}$ and irreversible volume changes $v^{(pl)}$ are linked together. This is usually expressed by the well-known phenomenological dilatancy constraint (Vardoulakis and Sulem, 1995)

$$\dot{v}^{(pl)} = d\left(g^{(pl)}\right)\dot{g}^{(pl)}, \qquad \dot{v}^{(pl)} = \dot{\varepsilon}_{kk}^{(pl)}; \tag{5.12}$$

$d\left(g^{(pl)}\right)$ is called the "mobilized dilatancy coefficient." That is to say, there is great class of deformations where there is no need to treat irreversible volume changes separately from irreversible shear deformations. Within the frame of nonassociative flow theory of plasticity one may chose the deviatoric plastic strain $\dot{g}^{(pl)}$ as the hardening parameter as proposed by Kachanov (1974), which can be interpreted as the average interparticle slip. This strain invariant may be expressed as follows,

$$\dot{g}^{(pl)} = \sqrt{2\dot{e}_{ij}^{(pl)}\,\dot{e}_{ji}^{(pl)}}, \qquad \dot{e}_{ji}^{(pl)} = \dot{\varepsilon}_{ji}^{(pl)} - \dot{\varepsilon}_{kk}^{(pl)}\delta_{ij}/3. \tag{5.13}$$

Thus, one may set

$$\Delta\psi \equiv \Delta g^{(pl)}. \tag{5.14}$$

3. Experimental Evidence

In this work we employ a database of uniaxial and triaxial compression experiments on Serena (or Firenzuola) sandstone intact cylindrical specimens with diameter $D = 5\,\text{cm}$ and height $H = 10\,\text{cm}$ that were performed at SINTEF (Norway). The mineralogical setup and basic physical properties of this type of sandstone are displayed in Table 5.1. In all the tests carried out in the frame of this work a certain number of unloading–reloading cycles were performed in order to study the elasticity of the test specimens. During its test the axial force (F), the engineering axial strain (ε_a), and the engineering radial (or lateral) strain (ε_r) were recorded by LVDTs and stored on a computer. The axial stress (σ_a) was computed from the formula

$$\sigma_a = \frac{F}{\pi D^2/4}. \tag{5.15}$$

For the cylindrical samples subjected to axial loading and under small strains the volumetric strain (ε_v) was computed from the formula

$$\varepsilon_v = (2\varepsilon_r + \varepsilon_a), \tag{5.16}$$

where ε_r and ε_a are the axial and radial strains, respectively.

As illustrated in Figure 5.3 the tested rock exhibits strong stress dependence of the elastic (unloading–reloading) curves, which are characterized by appreciable nonlinearity. Thus, the simple secant-modulus calibration procedure by virtue of relation (5.6) with rather linear unloading–reloading curves cannot be readily applied. Vardoulakis et al. (1998) developed a hypoelastic model for marble that accounts for stress dependency of the Young's modulus but assumes a constant Poisson ratio of the marble. In a next section a new hypoelastic model based on damage mechanics is developed that considers as variables a secant elastic modulus and Poisson ratio of intact rocks.

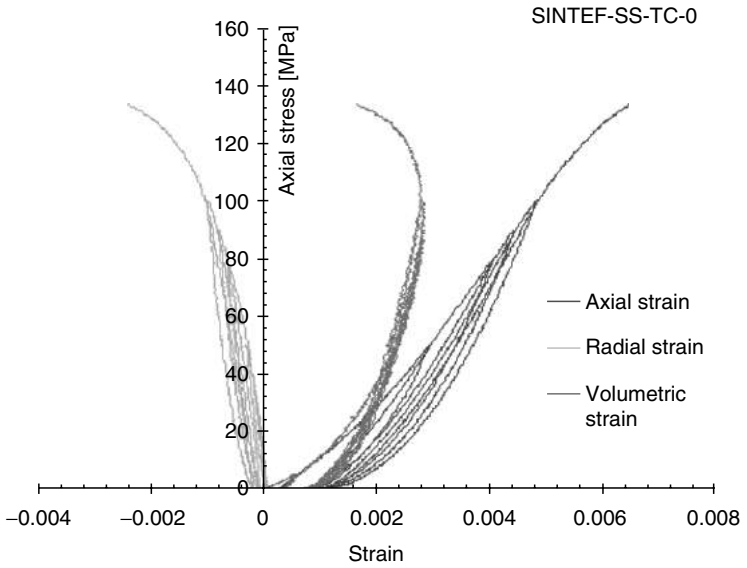

Fig. 5.3. Axial stress versus axial, radial, and volumetric strains for Serena sandstone specimen SS-TC-0 at zero confining stress (courtesy of E. Papamihos)

Table 5.1. Mineralogical and petrophysical properties of the tested Serena sandstone

Mineral or physical property	Serena (Firenzuola) sandstone
Calcite [%]	21 – 8
Dolomite [%]	7 – 0
Quartz [%]	32 – 36
Potassium Feldspar [%]	7
Plagioclase [%]	13 – 15
Phylosilicates [%]	20 – 34
Total porosity [%]	9.76
Bulk density $[Mg/m^3]$	2.57

In the sequel, the observed mechanical behavior of sandstone in Uniaxial Compression (UC) and Triaxial Compression (TC) is described with simple mathematical relations. Note that in this section we deviate momentarily from the assumed stress sign convention and we assume compressive stresses as positive. First, by considering only the loading branch of the UC data, the path of a rock sample to failure can be followed by plotting the measured axial and radial strains versus the applied axial stress. For example, the graphs of axial stress versus axial strain and radial strain versus axial strain for the uniaxial compression test SS-TC-0 are displayed in the Figures 5.4a and b, respectively. We remark here that the high unconfined compressive strength exhibited by this sandstone is due to the high content of quartz (see Table 1). The data taken from primary loading loops are fitted by polynomials of the form

$$\begin{aligned} \sigma_a &= a_1 x + a_2 x^2 + a_3 x^3 + \cdots , \\ 1000 \cdot \varepsilon_r &= b_1 x + b_2 x^2 + b_3 x^3 + \cdots , \\ x &= 1000 \cdot \varepsilon_a . \end{aligned} \tag{5.17}$$

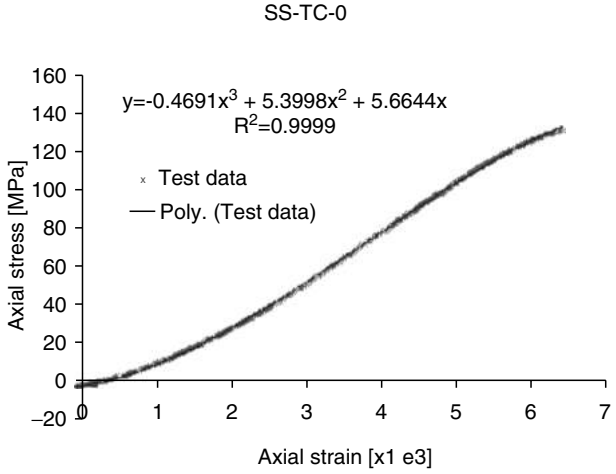

Fig. 5.4. Loading branches of (a) axial stress–axial strain and (b) radial strain–axial strain curves of Serena sandstone specimen SS-TC-0 in UC and fitted polynomial curves.

The nonlinearity of sandstone is manifested by the dependence of the tangent modulus of deformability and lateral strain factor on the applied stress. In fact, differentiating formulae (5.17) with respect to x or ε_a we obtain the following expression for the tangent moduli,

$$\begin{aligned} E_t &= \frac{\partial \sigma_a}{\partial \varepsilon_a} = a_1 + 2a_2 x + 3a_3 x^2 + \cdots, \\ \nu_t &= -\frac{\partial \varepsilon_r}{\partial \varepsilon_a} = -b_1 - 2b_2 x - 3b_3 x^2 + \cdots. \end{aligned} \tag{5.18}$$

In the case of test SS-TC-0 six unloading–reloading cycles were performed before the peak stress at failure in order to infer its elastic properties. From the graphs displayed in Figures 5.5a,b it may be observed that the unloading–reloading curves corresponding to $\sigma_a - \varepsilon_a^{(el)}$ and to $\varepsilon_r^{(el)} - \varepsilon_a^{(el)}$ display nonlinearity and hysteresis. Neglecting hysteresis for the sake of simplicity, each of these loops is best-fitted by second-degree polynomials.

The recorded peak stresses during the four uniaxial and triaxial compression tests are plotted in Figure 5.6a in the form of Mohr circles; that is,

$$\sigma = \frac{\sigma_1 + \sigma_3}{2} + \frac{\sigma_1 - \sigma_3}{2} \cos 2\theta, \quad \tau = \frac{\sigma_1 - \sigma_3}{2} \sin 2\theta, \tag{5.19}$$

wherein σ_1, σ_3 denote the principal stresses at failure (i.e., axial and confining, respectively) and θ is the angle subtended between the horizontal line and the outward normal to the plane in which the normal and shear stresses (σ, τ), respectively, act. According to the celebrated Mohr–Coulomb (MC) linear failure criterion (Jaeger and Cook, 1976),

$$|\tau| = c + \tan\varphi\sigma, \tag{5.20}$$

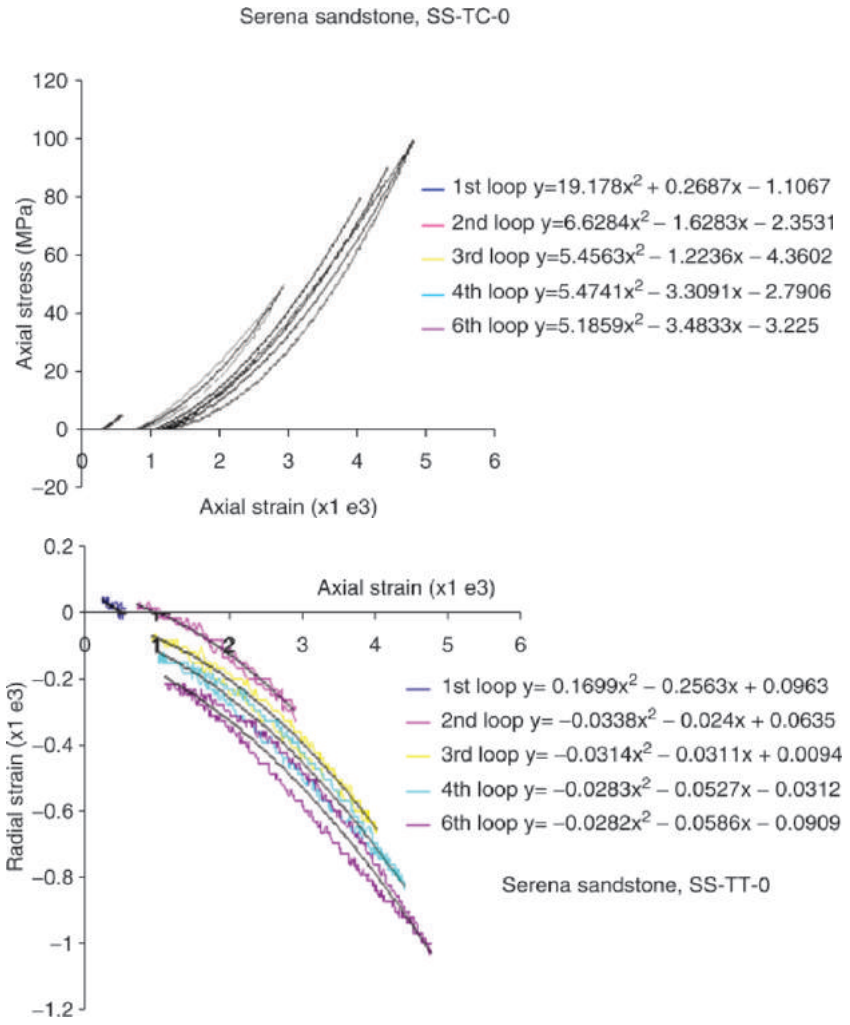

Fig. 5.5. Unloading–reloading loops for Serena sandstone in UC: (a) $\sigma_a - \varepsilon_a^{(el)}$, (b) $\varepsilon_r^{(el)} - \varepsilon_a^{(el)}$.

where the cohesion c and the internal friction angle φ of Serena sandstone are derived by passing a straight line that is tangent to all Mohr circles (e.g., Figure 5.6a). The values of these properties have been found to be c = 23.5 MPa and $\varphi = 53°$. The photos in Figure 5.6b illustrate the failure modes exhibited by three sandstone specimens subjected to different confining pressures. The high friction angle of the sandstone is manifested with the low angle subtended between the vertical axis and the shear crack exhibited by the specimens at the moment of failure[2] (Figure 5.6b).

[2] As is well known this angle denoted by the symbol β is given by $\beta = \pi/4 - \varphi/2$.

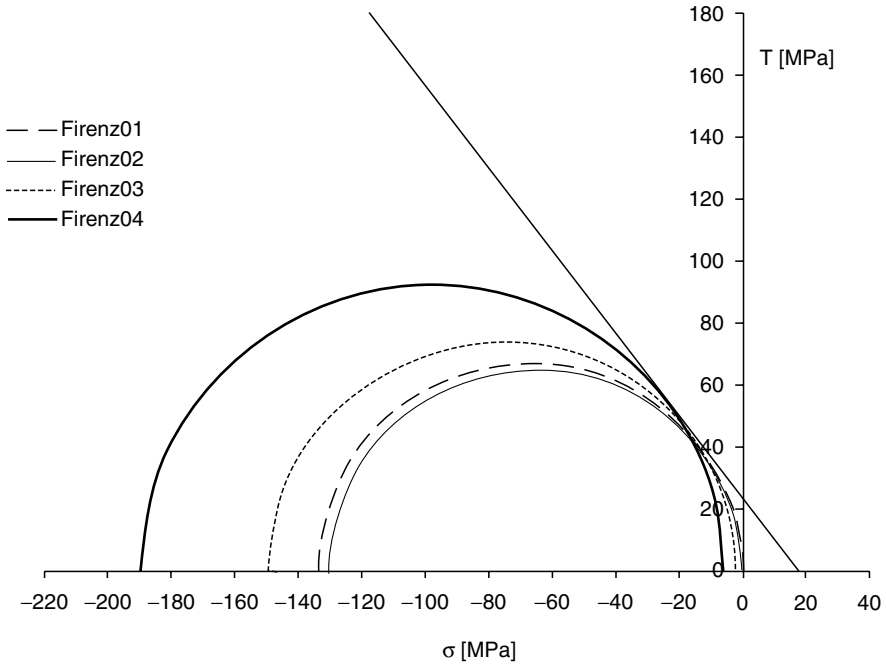

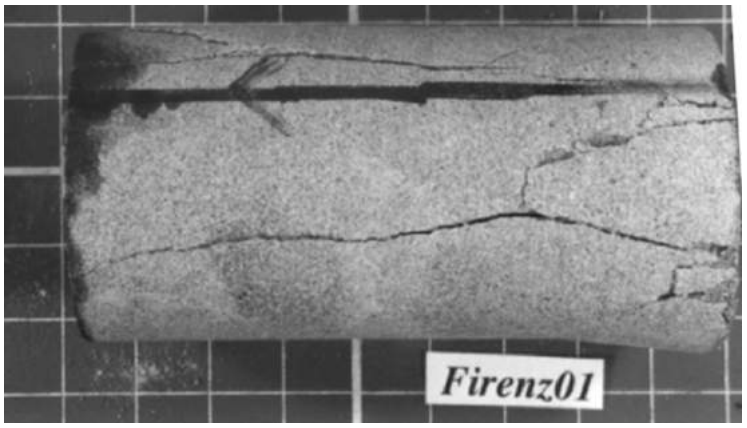

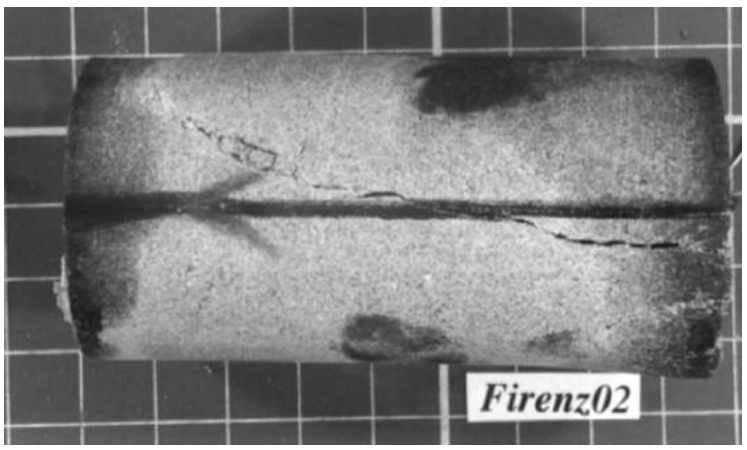

Fig. 5.6. Continued.

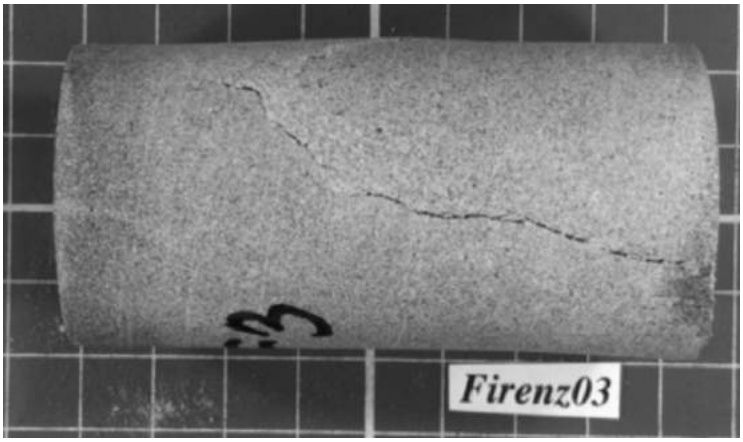

Fig. 5.6. (a) Mohr circles and fitted linear Mohr–Coulomb failure envelope; (b) photos of sandstone cylindrical specimens broken in uniaxial and triaxial compression tests (courtesy of E. Papamihos).

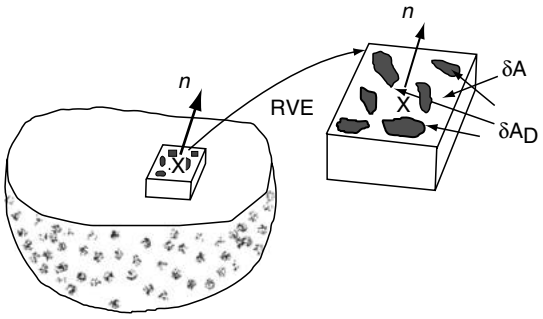

Fig. 5.7. Representative Elementary Volume (REV) of damaged rock.

4. Calibration of a Nonlinear Model on Experimental Data

4.1 A Hypoelastic-Damage Model for Sandstone

In this section a new hypoelastic theory for intact rocks is developed to account for this stress dependency of both elastic moduli of Serena sandstone found in the experiments.

Elasticity of intact rocks is determined by the elastic stiffness of the uncracked rock and the geometry (density and orientation) of microcracks. It may be assumed that the geometry of microcracks—which may be approximated in any plane by the area of intersections of cracks with that plane—can be modeled through a continuum variable at the mesoscale (i.e., grain scale). In order to manipulate a dimensionless quantity the crack area δA_D is scaled with the size of the area of the Representative Elementary Volume (RVE). This size is of primary importance in the definition of a continuous variable in the sense of continuum mechanics. This continuum damage variable is similar to the plastic strain of classical plasticity that at a given point represents the average of many grain slips.

If the area δA with outward unit normal n_j of the RVE with position vector x_i of Figure 5.7 is loaded by a force δF_i the usual apparent traction vector $\sigma_i = \sigma_{ij} n_j$ is

$$\sigma_i = \lim_{\delta A \to S} \frac{\delta F_i}{\delta A}, \quad i = 1, 2, 3, \tag{5.21}$$

where S is the representative area of the intact rock. The value of the dimensionless damage quantity $D(n_i, x_i)$ may be defined as follows,

$$D = \frac{\delta A_D}{\delta A}. \tag{5.22}$$

At this point we may introduce an effective traction vector $\sigma_i^{(e)}$ that is related to the surface that effectively resists the load, namely,

$$\sigma_i^{(e)} = \lim_{\delta A \to S} \frac{\delta F_i}{\delta A - \delta A_D}, \quad i = 1, 2, 3. \tag{5.23}$$

From relations (5.21)–(5.23) it follows that

$$\sigma_i^{(e)} = \frac{\sigma_i}{1 - D}, \quad i = 1, 2, 3. \tag{5.24}$$

According to the above definitions the elastic deformation of the intact rock can be described with the following relations.

- The relation $\sigma_{ij}^{(e)} - \varepsilon_{ij}^{(el)}$ which is obtained from elasticity
- The relation $\sigma_i - \sigma_i^{(e)}$ which is obtained by employing the concept of damage (Lemaitre, 1992).

It is convenient to decompose the stress tensor σ_{ij} into deviatoric and hydrostatic parts as follows,

$$\sigma_{ij} = s_{ij} + p\delta_{ij}, \tag{5.25}$$

wherein s_{ij} denotes the stress deviator and $p = \sigma_{kk}/3$ is the mean pressure. Furthermore, we introduce the stress invariants

$$I_{1\sigma} = \sigma_{kk}, \quad J_{2s} = \frac{1}{2} s_{ij} s_{ji}, \tag{5.26}$$

wherein $I_{1\sigma}$ is the first invariant of the spherical stress tensor and J_{2s} is the second invariant of the deviatoric stress tensor. The generalization of damage theory in three dimensions may be performed by assuming that microcracks and pores reduce[3] the apparent distortional and hydrostatic intensities of the stress tensor according to the relations

$$I_{1\sigma} = (1 - D_s) \cdot I_{1\sigma}^{(e)}, \quad T = (1 - D_c) \cdot T^{(e)}, \tag{5.27}$$

[3] It may be noted here that a general theory must allow for both enhancement and degradation of material properties due to mechanical loads. The former case corresponds to negative damage measures and describes pore and microcrack closure (healing) due to hydrostatic pressure and the latter corresponds to positive damage measures and describes microcrack opening and propagation. Both degradation and enhancement of the properties of a solid may be embraced under the term "material divagation" that is used to describe processes where the mechanical properties of a material change in time or wander from the values that characterize the material in a reference configuration. In general, divagation can result from any thermal, mechanical, chemical, or electrical process experienced by the material.

where $T = \sqrt{J_{2s}}$ denotes the deviatoric shearing stress intensity. In the above relations it is assumed that the scalar damage variables D_s, D_c are the spherical (hydrostatic) and distortional intensities of the damage tensor D_{ij}, respectively. From relations (5.25) and (5.27) the apparent versus the effective stress tensor relationship may be obtained:

$$\sigma_{ij} = (1 - D_c) \cdot \sigma_{ij}^{(e)} + \frac{1}{3} \cdot (D_c - D_s) \cdot \delta_{ij} \cdot \sigma_{kk}^{(e)}. \tag{5.28}$$

Next, we recall the finite-elasticity equations for the volumetric and deviatoric strains

$$\varepsilon_{kk}^{(el)} = \frac{p}{K_s} \; ; \; e_{ij}^{(el)} = \frac{s_{ij}}{2G_s} \tag{5.29}$$

and

$$e_{ij}^{(el)} = \varepsilon_{ij}^{(el)} - \frac{1}{3}\delta_{ij}\varepsilon_{kk}^{(el)}, \tag{5.30}$$

where K_s is the secant bulk modulus and G_s is the secant shear modulus of the rock material that are related to the secant Young modulus E_s and Poisson ratio ν_s through the formulae

$$K_s = \frac{E_s}{3(1 - 2\nu_s)}, \quad G_s = \frac{E_s}{2(1 + \nu_s)}. \tag{5.31}$$

Alternatively, we may also find the relations,

$$\nu_s = \frac{3K_s - 2G_s}{2(3K_s + G_s)}, \quad E_s = \frac{9\ K_s\ G_s}{3K_s + G_s}. \tag{5.32}$$

Equations (5.27) and (5.29) lead to the following relations,

$$K_s = K_0\,(1 - D_s)\,, \quad G_s = G_0\,(1 - D_c)\,. \tag{5.33}$$

From (5.29) and (5.30) one may derive rate-type elasticity (hypoelasticity) equations that are obtained through formal material time differentiation

$$\dot{p} = K_s \dot{\varepsilon}_{kk}^{(el)} + p\frac{\dot{K}_s}{K_s}; \quad \dot{s}_{ij} = 2G_s \dot{e}_{kk}^{(el)} + s_{ij}\frac{\dot{G}_s}{G_s}, \tag{5.34}$$

where $e_{ij}^{(el)}$ denotes the elastic strain deviator, and $\varepsilon_{kk}^{(el)}$ is the elastic volumetric strain. By recourse to formal differentiation of formulae (5.38)

$$\frac{\dot{K}_s}{K_s} = -\frac{\dot{D}_s}{1 - D_s}; \quad \frac{\dot{G}_s}{G_s} = -\frac{\dot{D}_c}{1 - D_c} \tag{5.35}$$

and relations (5.28) we extract the relation between the apparent stress and the elastic strain increments

$$\dot{\sigma}_{ij} = 2G_s \dot{\varepsilon}_{ij}^{(el)} + \left(K_s - \frac{2}{3}G_s\right)\,\delta_{ij}\,\dot{\varepsilon}_{kk}^{(el)} - s_{ij}\frac{\dot{D}_c}{1 - D_c} - p\,\delta_{ij}\frac{\dot{D}_s}{1 - D_s}. \tag{5.36}$$

The above incremental expression may be set into the equivalent compact form

$$\dot{\sigma}_{ij} = C_{ijkl}^{(el)} \dot{\varepsilon}_{kl}^{(el)}, \tag{5.37}$$

where $C_{ijkl}^{(el)}$ is the "tangent elastic stiffness matrix" that according to the above damage model is now an anisotropic fourth rank tensor.

4.2 A Plasticity Model for Sandstone

Herein it is assumed that the "isotropic hardening rule" of rocks in compression is the same as that in tension. That is, past the initial yield state, friction is mobilized and increases as a function of plastic shear strain until it reaches saturation at some peak value. This friction-hardening phase is consequently described as an isotropic hardening phase as shown in Figure 5.8 [state i (initial yield) to state f (failure)] in which q is the strength of the uncracked rock matter (it is called *tensile limit* of the material).

The yield curves for this model are linear with their slopes to be steeper than the initial i yield curve. This is expected because the mean orientation of the active cracks $f(g^{(pl)})$ is changing as the rock proceeds from initial yield to failure according to the rough model of Figure 5.9. Thus $f\left(g^{(pl)}\right)$ represents a stress orientation coefficient in terms of fracture mechanics or a friction coefficient in terms of MC yield criterion.

For the calibration of the MC yield surface based on the UC test results:

$$F = \sqrt{J_{2s}}\left[\sin\left(\alpha_{so} + \frac{\pi}{3}\right) + \frac{1}{\sqrt{3}}\cos\left(\alpha_{so} + \frac{\pi}{3}\right)\sin\varphi_m\right] - \left(q - \frac{1}{3}I_{1\sigma}\right)\sin\varphi_m = 0, \tag{5.38}$$

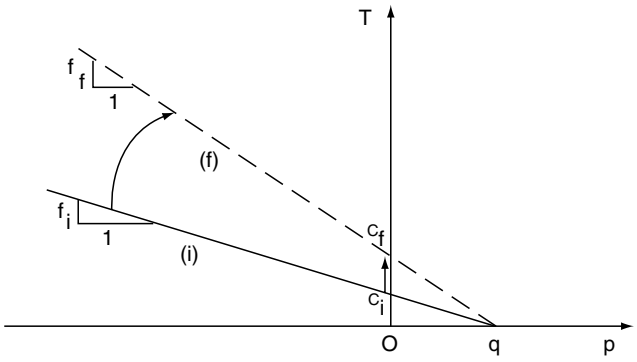

Fig. 5.8. Motion of the yield surface in $(T-p)$ stress space. $(i-f)$ isotropic friction hardening phase with constant q.

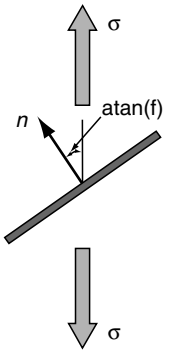

Fig. 5.9. Physical meaning of the stress inclination parameter f, that is, the angle subtended between the outward unit normal vector n on a straight microcrack with the tensile (or compressive) stress (σ) axis.

where α_{so} is the stress invariant angle of similarity (i.e., the third stress invariant), we set $\alpha_{so} = \pi/3$ (Chen and Han, 1988) which means

$$F = 0 \;\Leftrightarrow\; T\left(\frac{\sqrt{3}}{2} - \frac{1}{2\sqrt{3}}\sin\varphi_m\right) - (q - p)\sin\varphi_m = 0, \tag{5.39}$$

with the mean normal stress defined as follows (compressive stresses assumed here negative)

$$p = \frac{1}{3}(2\sigma_r + \sigma_z) \quad \Rightarrow \quad p = \frac{1}{3}(-\sigma_a). \tag{5.40}$$

The friction coefficient is denoted by the symbol f_c and is defined by the ratio

$$F = 0 \quad \Rightarrow \quad f_c = \frac{T}{q - p}. \tag{5.41}$$

The mobilized internal friction angle ϕ_m and the mobilized cohesion c_m for the constant q MC-model read as follows

$$\sin\phi_m = \frac{3f_c}{2\sqrt{3} + f_c}, \quad c_m = q\tan\phi_m. \tag{5.42}$$

4.3 Constitutive Elastoplastic Model of Serena Sandstone

Returning to the sandstone UC test, in the uniaxial compression case we have (assuming compressive stresses as positive)

$$p = \frac{1}{3}\sigma_a, \quad s_a = \frac{2}{3}\sigma_a, \quad s_r = -\frac{1}{3}\sigma_a \tag{5.43}$$

and the incremental stress–strain relations (5.36) take the form

$$\begin{aligned} d\sigma_a &= 2G_s d\varepsilon_a^{(el)} + \left(K_s - \tfrac{2}{3}G_s\right)\left(d\varepsilon_a^{(el)} + 2d\varepsilon_r^{(el)}\right) \\ &\quad -s_a\tfrac{\dot{D}_c}{1-D_c} - p\tfrac{\dot{D}_s}{1-D_s}, \\ 0 &= 2G_s d\varepsilon_r^{(el)} + \left(K_s - \tfrac{2}{3}G_s\right)\left(d\varepsilon_a^{(el)} + 2d\varepsilon_r^{(el)}\right) \\ &\quad -s_r\tfrac{\dot{D}_c}{1-D_c} - p\tfrac{\dot{D}_s}{1-D_s}. \end{aligned} \tag{5.44}$$

The empirical relations of bulk and shear secant moduli of Serena sandstone are derived from the unloading–reloading test data and the above relations (5.44) (Figure 5.10a). The two "enhancing" functions at hand may be approximated in first order for every loop by the linear relations

$$\begin{aligned} D_s\left(\varepsilon_a^{(pl)}\right) &= -41.5\left(\varepsilon_a^{(el)} - \varepsilon_a^{(pl)}\right), \\ D_c\left(\varepsilon_a^{(pl)}\right) &= -30\left(\varepsilon_a^{(el)} - \varepsilon_a^{(pl)}\right). \end{aligned} \tag{5.45}$$

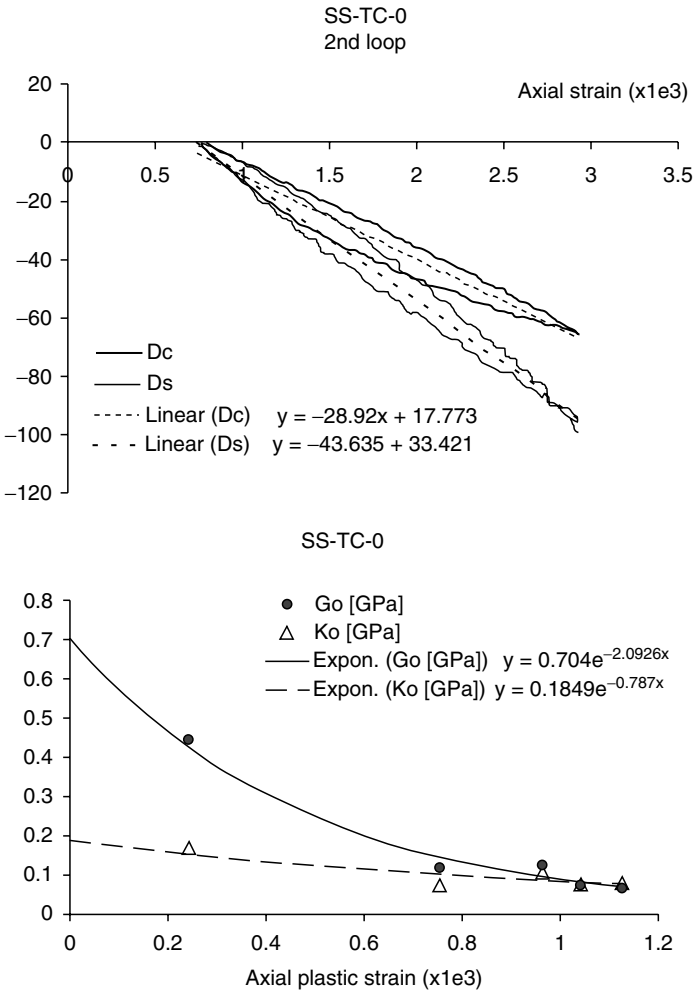

Fig. 5.10. (a) Dependence of damage scalar variables of sandstone on axial strain in the second loop, and (b) best exponential fit dependence of initial elastic moduli of each unloading–reloading loop on the axial plastic strain.

Then based on the above damage theory the moduli of sandstone were expressed as a function of the damage or enhancing functions as follows

$$\begin{aligned} K_s &= K_0\left(\varepsilon_a^{(pl)}\right)\left[\,1 - D_s\left(\varepsilon_a^{(pl)}\right)\,\right], \\ G_s &= G_0\left(\varepsilon_a^{(pl)}\right)\left[\,1 - D_c\left(\varepsilon_a^{(pl)}\right)\,\right], \end{aligned} \tag{5.46}$$

where the initial elastic moduli were found to be negative exponential functions of the axial plastic strain (Figure 5.10b),

$$\begin{aligned} K_0 &= 0.185\, e^{-0.787\,\varepsilon_a^{(pl)}}, \\ G_0 &= 0.704\, e^{-2.093\,\varepsilon_a^{(pl)}}. \end{aligned} \tag{5.47}$$

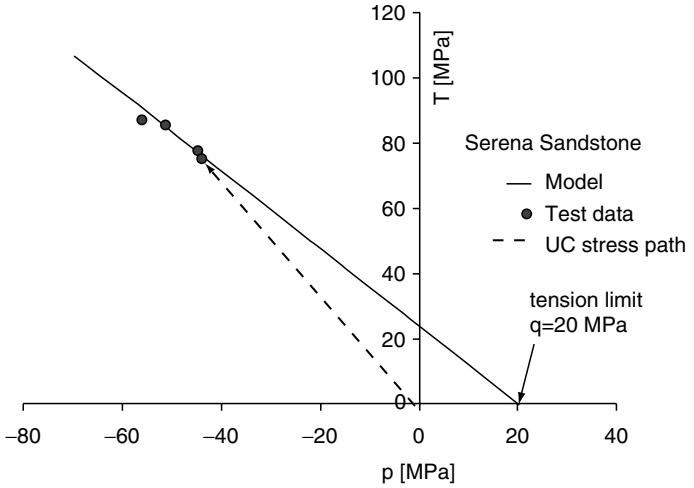

Fig. 5.11. Determination of the tension limit by best fitting a straight line on the uniaxial and triaxial compression test data at failure in the (p, T) stress space and UC stress path.

It is worth noticing that the above relations indicate that enhancement is linked or coupled with the plasticity exhibited by the sandstone.

The tension limit q of this type of the sandstone is found by fitting a straight line on the uniaxial and triaxial compression test data in the p-P space, as it is displayed in Figure 5.11. We can evaluate at each point of the stress–strain curves the plastic strains and plot the friction coefficient, the mobilized friction angle, and the mobilized cohesion as a function of the plastic shear strain intensity. The latter quantity is calculated as follows,

$$\dot{g} = \dot{g}^{(el)} + \dot{g}^{(pl)} = \frac{\dot{T}}{G} + \dot{g}^{(pl)} \quad \Rightarrow \quad \dot{g}^{(pl)} = \dot{g} - \frac{\dot{T}}{G}. \tag{5.48}$$

For the flow rule, by assuming coaxiality of stresses and strains, we employ a MC expression of the form

$$Q = T\left(\frac{\sqrt{3}}{2} - \frac{1}{2\sqrt{3}}\sin\psi_m\right) + p\ \sin\psi_m = 0. \tag{5.49}$$

Hence, the mobilized dilatancy angle ψ_m is calculated from the following relationship,

$$\sin\psi_m = \frac{3d}{2\sqrt{3} + d}. \tag{5.50}$$

An algorithm has been constructed based on the set of equations (5.44)–(5.47) describing the elasticity of the rock, as well as the set of equations (5.7)–(5.14), (5.17), (5.18), (5.38)–(5.42) and (5.48)–(5.50) describing its plastic behavior, in order to calculate the dependence of basic mechanical parameters on the amount of plastic shear strain intensity that is used as a load parameter. Figure 5.12 displays the dilation response, whereas Figure 5.13 shows the typical variation of the mobilized friction and

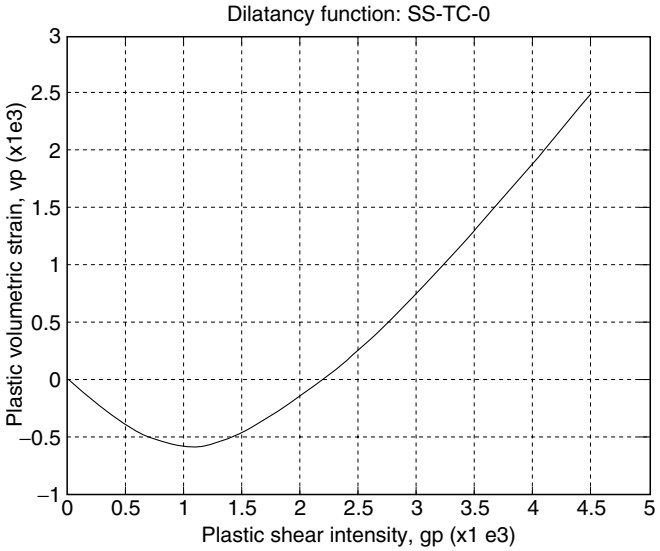

Fig. 5.12. Dilation response of Serena sandstone specimen SS-TC-0 in UC.

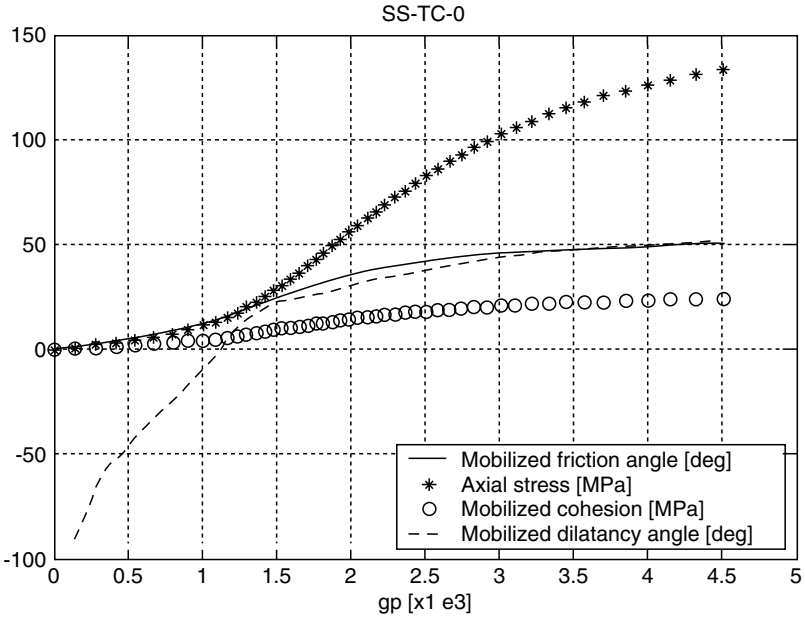

Fig. 5.13. Plots of mobilized friction and dilatancy angles, axial stress, and mobilized cohesion of Serena sandstone specimen SS-TC-0 in UC. The convention of compression positive is assumed.

dilatancy angles, cohesion, and axial stress as functions of the plastic shear strain intensity for the Serena sandstone, that are predicted by the assumed elastoplastic model. From the latter plot it may be seen that after some plasticity is developed in the specimen, the mobilized friction and dilatancy angles coincide, indicating an associated flow rule. Also, as was expected, the peak cohesion and peak internal friction angle

predicted by this model are in good agreement with the respective values of these strength properties derived from the linear MC failure envelope (e.g., Figure 5.6a.)

The predictability of the general model proposed above may be validated in a further step against additional test data (e.g., from the triaxial tests and tension tests or others). This validation procedure will reveal the weaknesses of the model that must be further elaborated in an iterative manner, until we obtain its most general applicability.

5. Summary and Conclusions

Carefully designed simple rock mechanics experiments performed on sandstone revealed their nonlinearity both in the elastic and plastic regimes. This necessitated the formulation of a nonlinear theory based on elasticity, damage mechanics, and plasticity theories. In a subsequent stage this theory was calibrated applying triaxial compression tests on Serena sandstone. Future work will include validation of the proposed model against more element or structural tests in the tensile and compressive regimes on the same type of stone. The hysteresis displayed by the sandstone was not considered in this first attempt. This is a topic of major interest that may be attacked by virtue of the theory of fracture mechanics in the near future. Fracture mechanics may also be used as a powerful tool to describe (a) the brittleness displayed by the rocks (i.e., their approximate tenfold decrease in compressive strength properties when they are subjected to tensile loads), and (b) the size effect that is manifested by the considerable reduction of their strength with the increase of the size of the structure. That is to say, modern rock mechanics should rely upon all the up-to-date developments of the fundamental theories of elasticity, strength of materials, damage mechanics, plasticity, and fracture mechanics in order to present robust models for rocks subjected to static or to dynamic loads. The linking of all these theories under the umbrella of a unique theory capable of describing the rock mechanical behavior at all scales (i.e., in the range 1e-6 m—1e 4 m) and boundary conditions encountered in praxis, is one of the fascinating challenges of the future.

Acknowledgments

This work is a result of research supported by funds of the MCDUR Project (G6RD-CT-2000-00266) and DIAS Project (DIAS-EVK4-CT-2002-00080) of the European Union.

References

Chen, W.F. and Han, D.J., 1988, *Plasticity for Structural Engineers*. Springer-Verlag, New York.

Frederick, D. and Chang, T.S., 1972, *Continuum Mechanics*, Scientific, Cambridge.

Guyer, R. and Johnson, P., 1999, Nonlinear mesoscopic elasticity: Evidence for a new class of materials, *Phys. Today*, 30–36.

Hill, R., 1950, *The Mathematical Theory of Plasticity*, Clarendon Press, Oxford.

Jaeger, J.C. and Cook, N.G.W., 1976, *Fundamentals of Rock Mechanics*, Chapman and Hall, London.

Johnson, P.A., 2005, Nonequilibrium non-linear dynamics in solids: State ofthe art in methods and applications, this volume.

Kachanov, L.M., 1974, *Fundamentals of the Theory of Plasticity*, MIR, Moscow.

Lemaitre, J., 1992, *A Course on Damage Mechanics* Springer-Verlag, Berlin.

Truesdell, C. and Noll, W., 1965, *The Non-Linear Field Theories of Mechanics*, Springer-Verlag, Berlin.

Vardoulakis, I. and Sulem, J., 1995, *Bifurcation Analysis in Geomechanics*, Blackie Academic & Professional, Berlin.

Vardoulakis, I., Kourkoulis, S.K. and Exadaktylos, G.E., 1998, Elasticity of marble, In *Recent Advances in Mechanics*, Kounadis A.N. & Gdoutos E.E. eds., Xanthi, Greece, July 10-12.